Cytological changes during luminescence production in lanternshark (Etmopterus spinax Linnaeus, 1758) photophores

Article *in* Zoomorphology · August 2014

DOI: 10.1007/s00435-014-0235-6

CITATIONS
4

READS
84

4 authors:

Marie Renwart
Université Catholique de Louvain
7 PUBLICATIONS **12** CITATIONS
SEE PROFILE

Jerome Delroisse
Université de Mons
42 PUBLICATIONS **47** CITATIONS
SEE PROFILE

Julien M Claes
30 PUBLICATIONS **244** CITATIONS
SEE PROFILE

Jérôme Mallefet
Université Catholique de Louvain
159 PUBLICATIONS **808** CITATIONS
SEE PROFILE

*Cytological changes during luminescence production in lanternshark (*Etmopterus spinax *Linnaeus, 1758) photophores*

Marie Renwart, Jérôme Delroisse, Patrick Flammang, Julien M. Claes & Jérôme Mallefet

Zoomorphology
Evolutionary, Comparative and Functional Morphology

ISSN 0720-213X

Zoomorphology
DOI 10.1007/s00435-014-0235-6

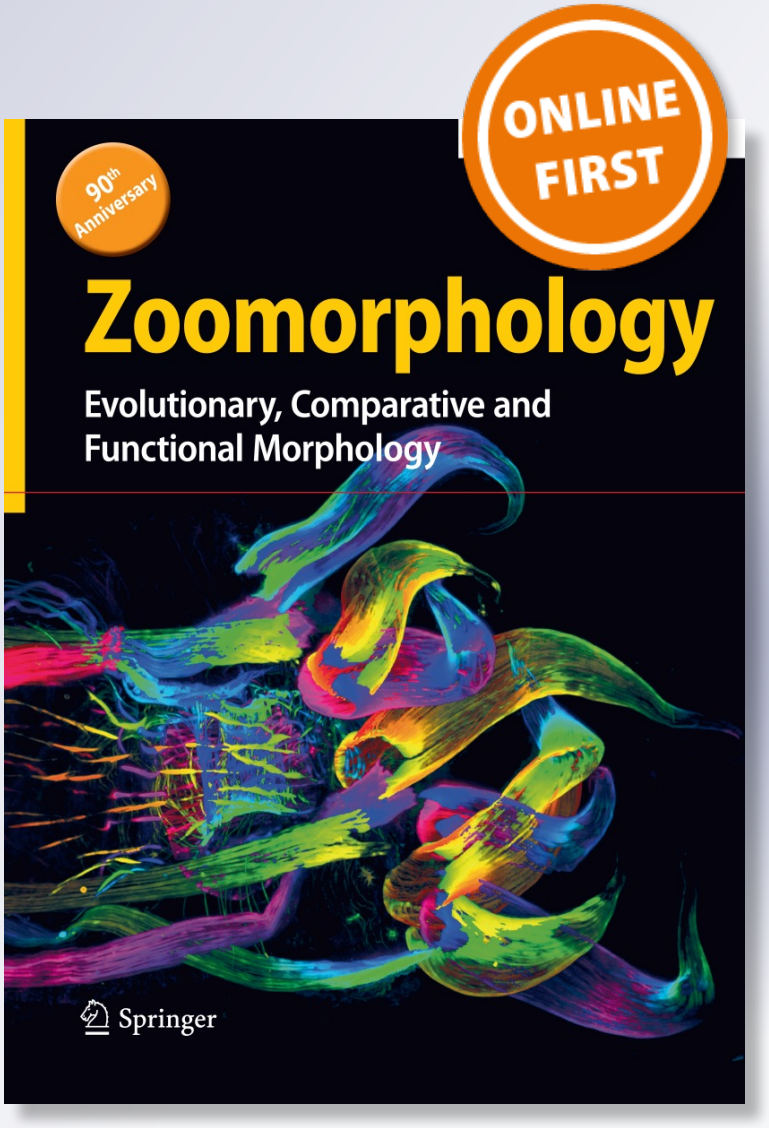

Springer

Zoomorphology
DOI 10.1007/s00435-014-0235-6

ORIGINAL PAPER

Cytological changes during luminescence production in lanternshark (*Etmopterus spinax* Linnaeus, 1758) photophores

Marie Renwart · Jérôme Delroisse · Patrick Flammang · Julien M. Claes · Jérôme Mallefet

Received: 13 May 2014 / Revised: 30 June 2014 / Accepted: 3 July 2014

Abstract Studying an organism's photogenic structures at the ultrastructural level is a key step in the understanding of its light-emission process. Recently, the photophore ultrastructure of the deep-sea lanternshark *Etmopterus spinax* Linnaeus, 1758 was described. The photocytes appeared to be divided into three areas including an apical granular area, which contains inclusions and was hypothesized to be the light-producing reaction site. In this study, we investigated the morphological changes occurring within the granular area during the bioluminescent emissions induced by two hormones: prolactin and melatonin. Prolactin provoked the formation of new structures in the granular area, the "grey particles", whose number was proportional to the amount of light produced by the reaction. An increase in the number of granular inclusions was also detected at the end of the prolactin-induced light emission. Conversely, melatonin induced a decrease in the number of granular inclusions and an increase in their diameter. An effect of hormones was also observed on the iris-like structure where they triggered pigment retraction and hence an increase in the iris aperture diameter. This is consistent with previous findings and is shown for the first time at the cellular level. The possible role of grey particles in *E. spinax* light-emission mechanism is discussed, while granular inclusion is considered to be *E. spinax*'s intracellular luminescence site. Regarding typical shark long-lasting glows, a new term ("glowon") is proposed to characterize this novel membrane-free microsource.

Keywords Chondrichthyes · Glowon · Melatonin · Microsource · Photocyte · Prolactin

Communicated by Andreas Schmidt-Rhaesa.

M. Renwart (✉) · J. M. Claes · J. Mallefet
Laboratory of Marine Biology, Earth and Life Institute, Catholic University of Louvain (UCL), Place Croix du Sud 3, bt L7.06.04, 1348 Louvain-la-Neuve, Belgium
e-mail: marie.renwart@uclouvain.be; marie.renwart@student.uclouvain.be

J. Delroisse · P. Flammang
Biology of Marine Organisms and Biomimetics, University of Mons (UMONS), Avenue du Champ de Mars 6, 7000 Mons, Belgium

Introduction

Etmopterus spinax Linnaeus, 1758 is a small deep-sea shark from the Etmopteridae family that displays bioluminescence on its ventral and lateral sides thanks to thousands of tiny light-emitting organs (photophores) (Claes and Mallefet 2008; Ebert et al. 2013). Etmopteridae and Dalatiidae are the only shark families containing known luminous members (Claes and Mallefet 2009a). Until recently, bioluminescence of sharks was poorly studied mainly due to their rarity and/or the relative inaccessibility of their deep-sea environment. In the past 6 years, *E. spinax* was used as a model species to study shark bioluminescence, as this shark can be easily obtained and maintained in captivity. Different aspects of shark luminescence, such as its ecological function (Straube et al. 2010; Claes et al. 2010a, 2013, 2014) and physiological control (Claes and Mallefet 2009b, 2010a, b; Claes et al. 2010b, 2011), are now better understood. Very recently, we described the ultrastructure of *E. spinax* photophores (Renwart et al. 2014), since it is a key step in the understanding of this shark's bioluminescence process. The photophores of *E. spinax* appear as cup-shaped organs composed of a protective layer of pigments (the pigmented sheath) and a reflector-like structure that encloses on

Published online: 02 August 2014

average 13 light-emitting cells (the photocytes), topped with different cell types including lens cells. Each photocyte is divided into three regions: the nucleus area, the vesicular area and the granular area. Because of its fluorescence capability, the presence of numerous granular inclusions as well as its particular orientation towards the photophore centre (Renwart et al. 2014), the granular area is believed to be the intracellular site of the luminous reaction (i.e. where light is produced). In this study, we aim to test this hypothesis by investigating the morphological changes occurring within the granular area during the light-emission process.

Materials and methods

Shark tissue collection

Specimens of *E. spinax* were collected by longlines in Norway (Raunefjord—60°15.908N; 05°07.778O) during two field missions, in November 2012 and March 2013. Sharks were killed according to the local rules for experimental fish care. Fresh ventral skin patches with photophores were dissected and placed in a buffered shark saline (Bernal et al. 2005) before the beginning of experiments.

Luminometry and electron microscopy

Skin patches were stimulated by two hormones (prolactin and melatonin) and fixed in glutaraldehyde at different stages of the light-emission process to be further observed in transmission electron microscopy. Four skin patches were dissected from each specimen and a total number of six sharks were used. One skin patch from each specimen was fixed before hormonal stimulation in a glutaraldehyde solution (3 % glutaraldehyde, 0.1 M sodium cacodylate, 0.27 M sodium chloride; pH 7.8) and was used as a control patch, the "*time 0*" sample. The remaining three patches were placed in chambers filled with 200 µl of hormone solution, either prolactin (10^{-6} M prolactin in a buffered shark saline; two patches) or melatonin (10^{-6} M melatonin in the same buffered shark saline; a single patch). The induced light was recorded during 1 h in a multiplate luminometer (Orion, Berthold Detection System, Pforzheim, Germany) connected to a computer. Consistent with previous findings (Claes and Mallefet 2009b), both hormones showed different light-emission pattern: prolactin induced a monophasic light curve that reached a peak after ~20 min and lasted a maximum of 60 min (Fig. 1); prolactin-stimulated skin patches were glutaraldehyde-fixed at the level of the peak ("PRL *max*") and 1 h after the stimulation start ("PRL *60*"). The melatonin-induced light curve reached a plateau after ~45 min and lasted over 60 min (Fig. 1); melatonin-stimulated skin patch was glutaraldehyde-fixed after 1 h ("MT *60*").

Fixed skin patches were processed using the method described in Renwart et al. (2014), in order to be observed in a transmission electron microscope (Zeiss Leo 906E). Briefly, skin patches were first decalcified (OsteoRAL R fast decalcifier, RAL diagnostics), and then post-fixed in osmium tetroxide (1 % osmium tetroxide, 0.1 M sodium cacodylate, 0.27 M sodium chloride; pH 7.8—45 min). Dehydrated patches were embedded in a Spurr's resin (10 g ERL 4206 resin, 6 g DER 736 resin, 26 g nonenyl succinic anhydride, 0.4 g dimethylaminoethanol), and sections of 90–110 nm were obtained using an ultramicrotome (Leica Ultracut UCT—Leica Microsystems) and placed on copper grids. Sections were finally contrasted in uranyl acetate [0.18 M uranyl acetate solution:ethanol (2:1)—45 min] and lead citrate (0.08 M lead nitrate, 0.12 M sodium citrate, 0.16 M sodium hydroxide—4 min) before observation.

Data analysis

Micrographs of hormonally stimulated photophores (*time 0*, PRL *max*, PRL *60* and MT *60*) were analysed using Image J v. 1.46 (National Institutes of Health, Bethesda, USA). Particular attention was given to the morphological changes occurring within the granular area of the photocytes, which may contain up to two distinct components, i.e. the "granular inclusions" and the "grey particles". Granular inclusions were analysed using three morphological parameters: the mean diameter, the density (per square micrometre) and the coverage (i.e. the percentage of the granular area surface occupied by granular inclusions). The first two parameters were calculated using the *watershed* followed by the *particle analysis* options of Image J. The total surface area of inclusions, required for the third parameter calculation, derived from the number of pixels was represented on the micrograph and not from the *particle analysis*, in order to allow direct comparison with the grey particles coverage. Indeed, only the coverage parameter was calculated for the grey particles, using the number of pixels, since these particles are very small and aggregate in a way that the *watershed/particle analysis* option cannot discriminate them. Both structures (granular inclusions and grey particles) have been analysed separately when present on the same micrograph by adjusting the threshold in binarized micrographs: a threshold of 80 was assumed to separate the darker granular inclusions from the lighter grey particles.

Statistical analyses were performed to investigate the evolution of the three parameters during the light-emission process. For each parameter, the two time points (i.e. *time 0* and MT *60*) of the melatonin-induced light curve and the

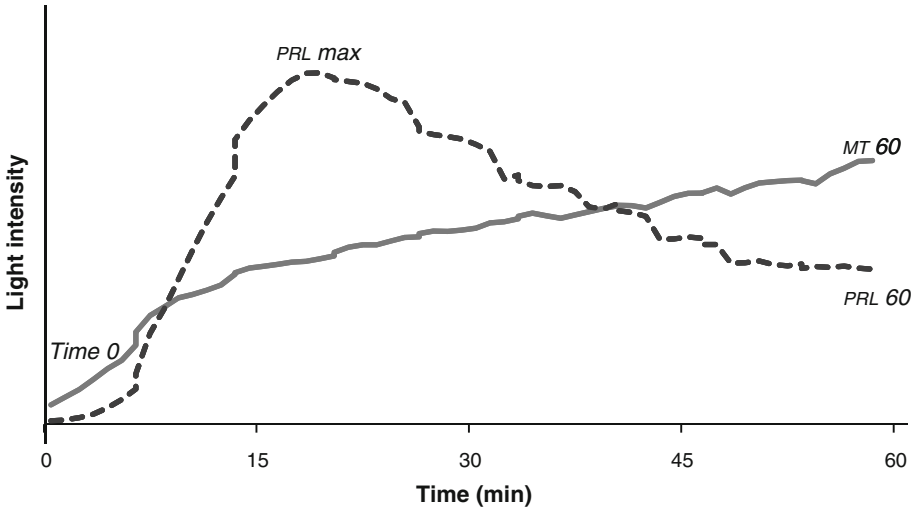

Fig. 1 Prolactin (*dashed line*) and melatonin (*grey line*)-induced light curves with associated time points

three time points (i.e. *time 0*, *PRL max* and *PRL 60*) of prolactin-induced light curve were compared using Student's *t* tests. Normality and equality of variance were tested by Shapiro–Wilk tests and Levene's tests, respectively. When one or both of these parametric assumptions could not be met, the Student's *t* tests were replaced by a Student's *t* tests on log-transformed data, a Welch's *t* tests or a Wilcoxon tests, respectively. All analyses were performed using the software JMP v. 11 (SAS Institute Inc., Cary, USA) and considered to be significant at the 0.05 level.

Results

Prolactin stimulation

A total of 125 photocytes (*time 0*, $N = 44$; *PRL max*, $N = 41$; *PRL 60*, $N = 40$) from 32 photophores (*time 0*, $n = 13$; *PRL max*, $n = 9$; *PRL 60*, $n = 10$) were used to investigate the ultrastructural changes induced by prolactin in *E. spinax* photogenic structures. Figure 2a shows three pictures of the granular areas of representative photocytes corresponding to the three analysed time points: at *time 0*, only the granular inclusions previously observed by Renwart et al. (2014) were visible. When the light emission reached its maximum (at *PRL max*), another structure appeared and was still present after 1 h, at *PRL 60*. We named it "grey particles", since their lower density to the electrons makes them appear lighter than granular inclusions.

Both granular inclusions and grey particles were quantified and compared between the three time points. The coverage of the grey particles showed a highly significant variation during the light-emission process (Fig. 2b). The coverage of the granular inclusions increased at the end of the light-emission process (Fig. 2c) as a significant difference between *PRL 60* and *PRL max* was obtained. The mean diameter of the inclusions did not change (Fig. 2d), but their density was significantly higher at *PRL 60* (Fig. 2e).

Stimulated photocytes presented overall a homogeneous distribution of both grey particles and granular inclusions (Fig. 3a–c); on few occasions, however, granular inclusions adopted a heterogeneous distribution, forming dense aggregations (clusters) in the granular area (Fig. 3d, e). Interestingly, most of these clustered inclusions were observed at *PRL max*. Moreover, it must be pointed out that different stages sometimes cohabited in a same photophore; indeed, a few photocytes at *PRL max* and *PRL 60* stages did not show the grey particles (Fig. 3a). Finally, endoplasmic reticulum was also observed surrounding groups of granular inclusions in a few stimulated photocytes (Fig. 3e, f).

Melatonin stimulation

A total of 92 photocytes (*time 0*, $N = 44$; *MT 60*, $N = 48$) from 26 photophores (*time 0*, $n = 13$; *MT 60*, $n = 13$) were used to investigate the ultrastructural changes induced by melatonin in *E. spinax* photogenic structures. Contrary to what was observed in prolactin-stimulated patches, melatonin did not appear to induce the formation of grey particles, since no grey particle coverage difference was observed either visually (Fig. 4a) or statistically (Fig. 4b) between the two time points. Similarly, the analyses did not reveal any significant difference between the two time points for the granular inclusions coverage (Fig. 4c). Inclusions were nevertheless found to have a significantly larger diameter and a significantly lower density at *MT 60* (Fig. 4d, e).

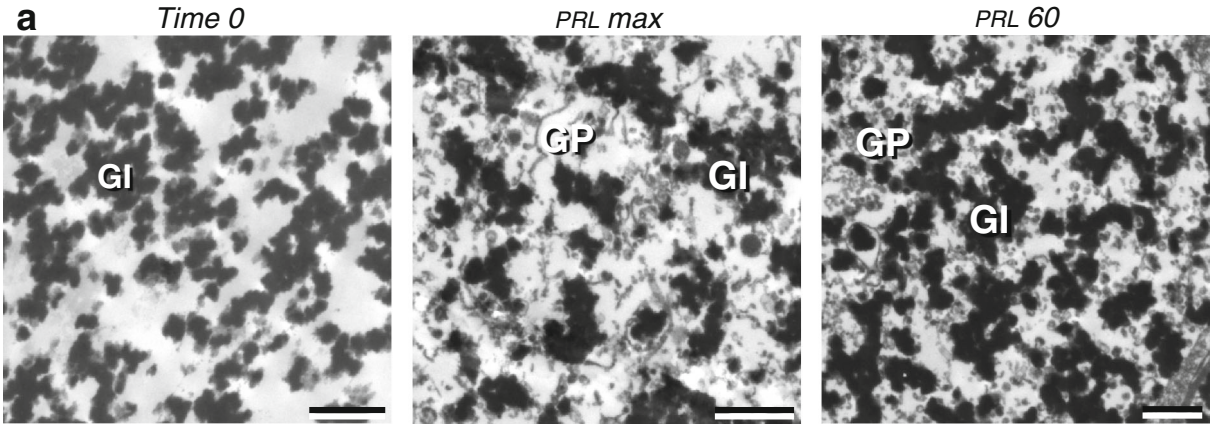

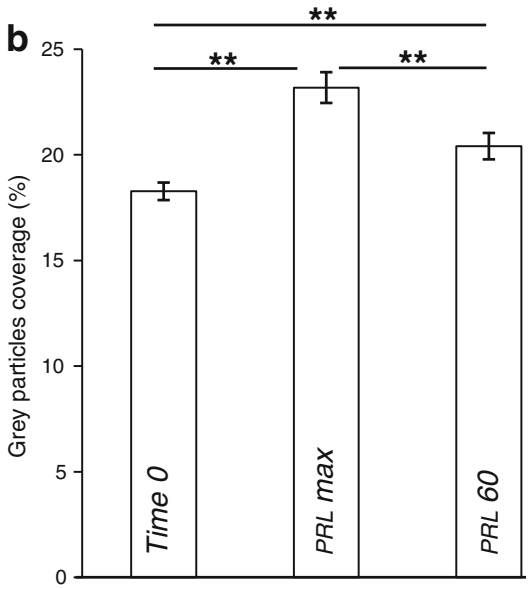

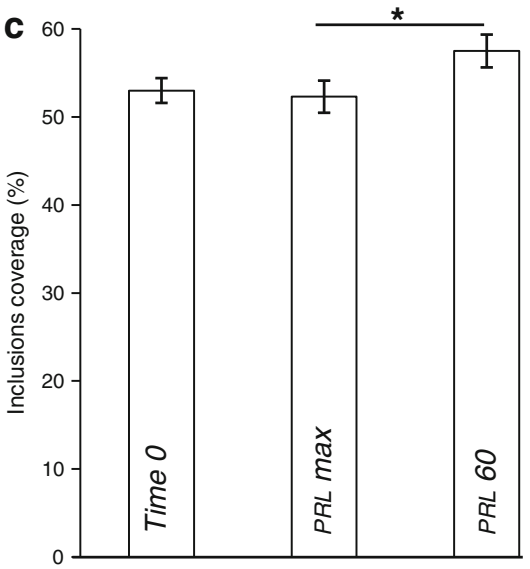

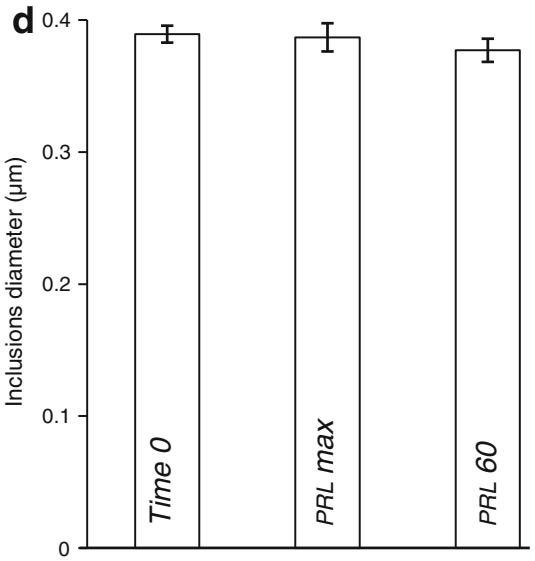

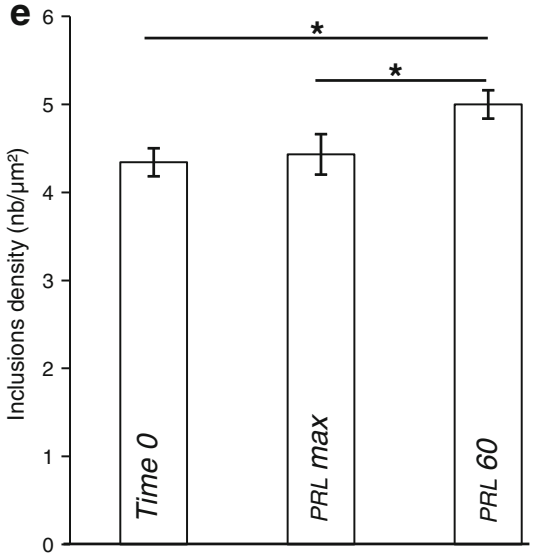

◀**Fig. 2** Prolactin-induced morphological changes in *E. spinax* photocytes. **a** Granular area at the three time points. *GI* granular inclusions, *GP* grey particles. *Scale bar* 1 µm. Photocyte morphological parameters at the three time points. **b** Grey particles coverage. **c** Granular inclusions coverage. **d** Granular inclusions diameter. **e** Granular inclusions density. *Asterisks* indicate statistically different means (*$P < 0.05$; **$P < 0.01$)

Iris-like structure aperture

An action of hormones was also observed at another photophore level. At *time 0*, melanosomes were present inside the photophore centre, forming the iris-like structure and surrounding the photocytes and their overlying cells. In stimulated photophores, pigments were removed from the photophore centre to form clusters around it, as illustrated in the Fig. 5 in a melatonin-stimulated patch.

Discussion

Morphological changes occurring in *E. spinax* photophore have been studied at the ultrastructural level throughout prolactin- and melatonin-induced light-emission processes. Both hormones are known to produce different light pattern (Claes and Mallefet 2009b). We found they also induced different morphological variations, either inside the photocytes or at the melanosomes level within the photophore. This brings further evidence of their different but complementary roles in the control of *E. spinax* luminescence (Claes and Mallefet 2009b, 2010b).

The main action of prolactin occurs inside the photocytes and primarily consists in the transitory formation of grey particles, while these particles were never observed in melatonin-stimulated photocytes. At *time 0*, the grey particle value only corresponds to the narrow edges of the granular inclusions, which appear grey on the black and white pictures (Fig. 2a), but no grey particles were observed at that stage. Grey particle coverage displays a monophasic development that follows the prolactin-induced light curve, reaching a maximum value at the light peak (at *PRL max*, Fig. 2b). This correlation clearly suggests an involvement of the grey particles in the light-emission process, although the exact nature of these particles, which might represent more than one component with the same electron density, cannot be attested in this study. Because grey particles only appear in prolactin-stimulated photocytes, they probably do not represent a constituent (reagent or product) of the chemiluminescent reaction, although we cannot completely rule out the grey particles to be a non-recycled product accumulating in prolactin-stimulated photocytes only. Very few luminous animals have been found with two different intrinsic luminescences (e.g. the Scyphozoan *Periphylla periphylla* Péron & Lesueur, 1810 and the teleost *Malacosteus niger* Ayres, 1848—Widder et al. 1984; Shimomura and Flood 1998), and in these cases, both luminescences were localized in different body parts and might involve the same light-emitting reaction. Occurrence of two light-emitting reactions in the same animal, and even more so in the same photogenic cell (one involving grey particles formation while the second do not), is very unlikely (Shimomura 2006). Therefore, we assume *E. spinax* photocytes to display one luminescence system and the grey particles to represent a component of the intracellular metabolic pathway, triggered by the binding of prolactin to its receptor, which consequently do not appear in melatonin-stimulated photocytes. Conversely, we assume granular inclusions—which are already present in the bioluminescence action site (i.e. the granular area) before prolactin stimulation— to be aggregations of stored/stabilized components (a substrate or a photoprotein, possibly combined with other molecular factors) waiting for a proper stimulus (possibly related to grey particles) to start the light-emitting reaction or increase the intensity of a basal emission.

Interestingly, both hormones showed a clear modification of the granular inclusions but acted on different parameters, arguing for their different roles in *E. spinax* light-emission process. Moreover, previous pharmacological experiments have shown an additive effect of both hormones on light intensity parameters (Claes and Mallefet 2009b), suggesting a close interaction at intracellular level in the shark photophore. In prolactin-stimulated photocytes, we found the granular inclusions to be more numerous after the reaction has been completed, which is also shown by their higher coverage at *PRL 60* (Fig. 2c, e). This higher density might reflect a restocking of reagents or an accumulation of products. In that context, non-activated photocytes at *PRL max* (i.e. showing no grey particles) might actually be recycling the products or rebuilding the reactive stock. This concept of a turnover of luminous material has already been proposed for another bioluminescent organism, the ophiuroid *Amphipholis squamata* Delle Chiaje, 1828 (Deheyn et al. 2000). In melatonin-stimulated photocytes, granular inclusions were found to have a significantly higher diameter 60 min after stimulation (at *MT 60*) concomitantly with a reduction in their density. This seems to indicate an aggregation of granular inclusions, since their coverage was shown to remain constant. Because melatonin induces a slow luminescence kinetics (Claes and Mallefet 2009b), effects of this hormone on photocyte ultrastructure may require a longer time to be clearly identified.

Variations in shape, number and size of cytoplasmic components related to bioluminescent activity have been demonstrated in various luminous organisms (Table 1). In

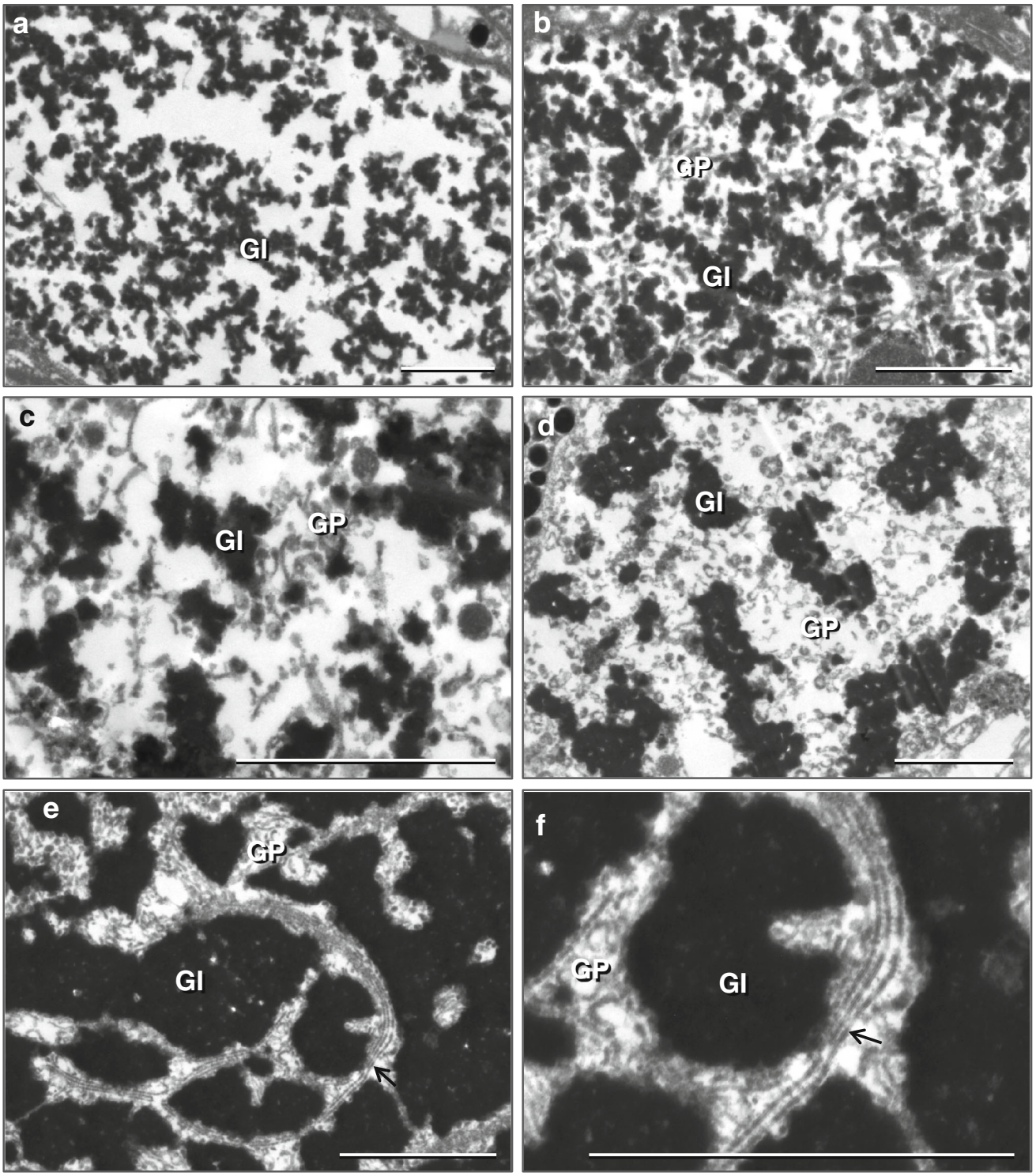

Fig. 3 Granular area from prolactin-stimulated photocytes. **a** A stimulated photocyte that does not show many grey particle. **b** Homogeneous distribution of granular inclusions. **c** Detailed view of the grey particles and the granular inclusions. Clustered distribution of granular inclusions at low (**d**) and high (**e**) density. **f** Higher magnification view of the endoplasmic reticulum (*arrows*) present in (**e**). *GI* granular inclusions, *GP* grey particles. *Scale bar* 2 μm

the ophiuroid *A. squamata*, the photocyte cytoplasm is full of vesicles that can be classified into six types (A–F). Only the vesicular type A is present before the luminous reaction, while type A, B and C are present during luminescence and mostly types D–F were seen after the reaction has been completed. Vesicular type A was assumed to

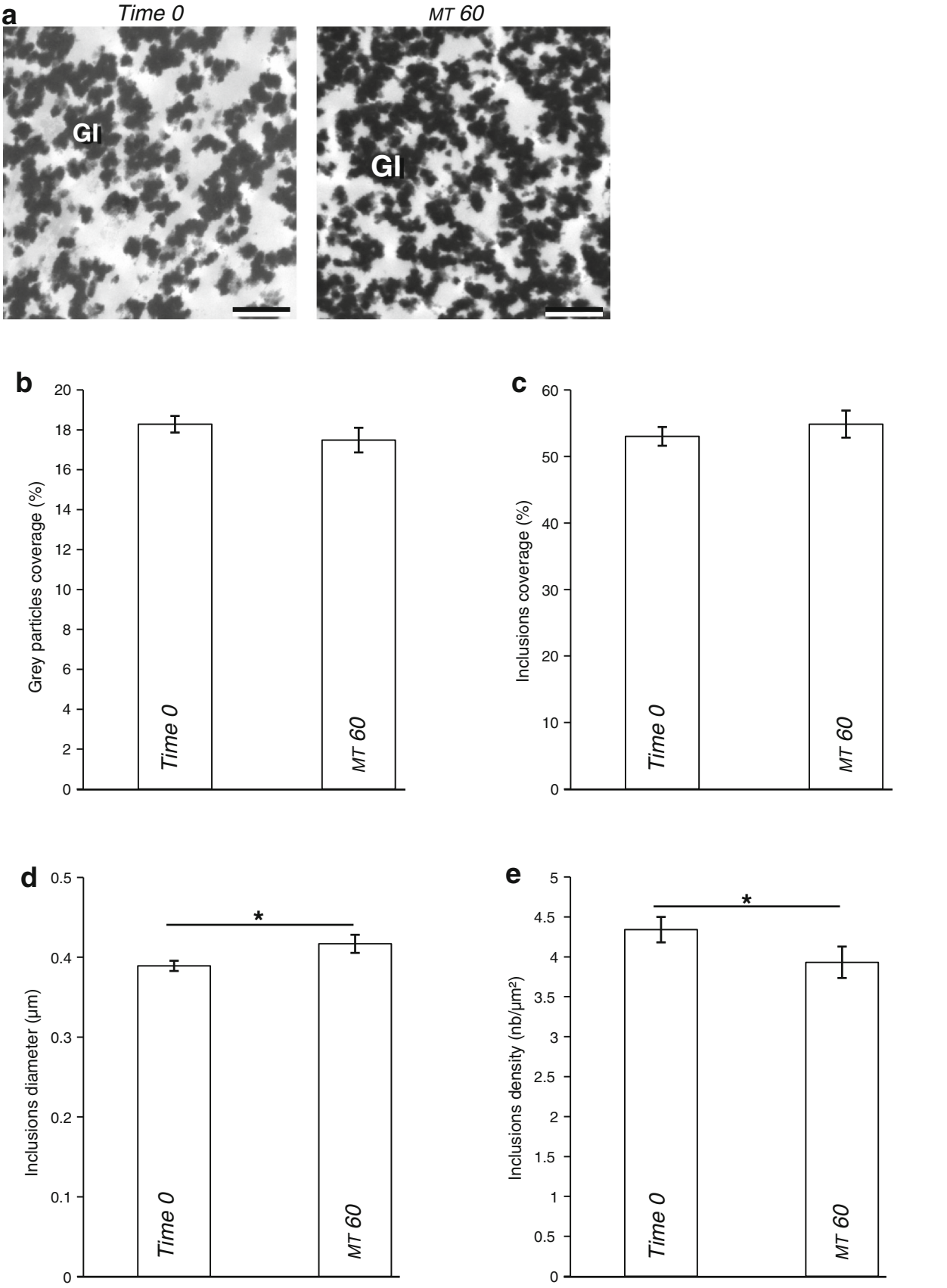

◀**Fig. 4** Melatonin-induced photocyte morphological changes. **a** Granular area at the two time points. *GI* granular inclusions. *Scale bar* 1 µm. Photocyte morphological parameters at the two time points. **b** Grey particles coverage. **c** Granular inclusions coverage. **d** Granular inclusions diameter. **e** Granular inclusions density. *Asterisks* indicate statistically different means ($*P < 0.05$)

contain one of the luminous component of the reaction, and the sequence of appearance of the other types allowed the authors to hypothesize the type C to be site of the luminous reaction (i.e. the microsource), further transformed into the type D at the end of the process (Deheyn et al. 2000). The midshipman fish *Porichthys notatus* Girard, 1854 also has a highly vesiculated cytoplasm subject to variations under injection of noradrenaline, a luminescence-triggering neurotransmitter in this species (Anctil 1979). Contrary to what occurs in many luminous organisms, *E. spinax* light-producing reaction does not take place in a membranous compartment of the photocyte but inside a specific region of the cytoplasm: the apical granular area. In this sense,

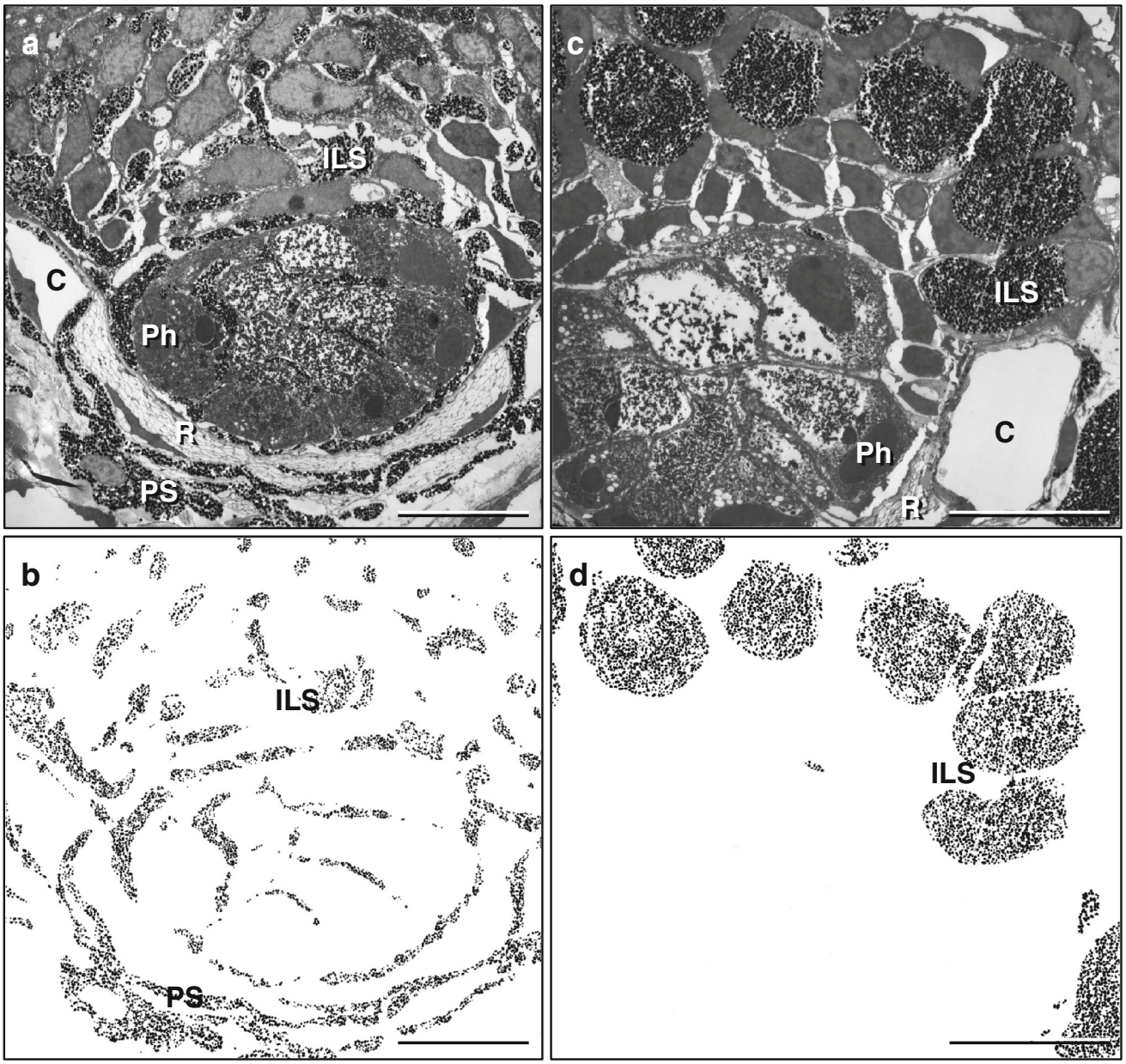

Fig. 5 Melatonin-induced pigment translocation. Whole structure (**a**) and pigment distribution (**b**) of a non-stimulated photophore. Whole structure (**c**) and pigment distribution (**d**) of a melatonin-stimulated photophore. Note the striking difference in the morphology of pigments, which adopt a clustered distribution in the iris-like structure after melatonin stimulation. *C* capillary, *ILS* iris-like structure, *Ph* photocyte, *PS* pigmented sheath, *R* reflector-like structure. *Scale bar* 20 µm

Table 1 Representative luminous species with corresponding microsource name, type and identification method

Taxa/selected species	Name	Type	Method
Dinoflagellata			
Lingulodinium polyedrum J. D. Dodge, 1989	Scintillons	Cytoplasmic granular structures	Microsources isolation, electron microscopy[1]
Cnidaria			
Renilla reniformis Pallas, 1766	Lumisomes	Membranous organelles	Microsources isolation, electron microscopy[2]
Annelida, Polychaeta			
Acholoe squamosa Delle Chiaje, 1827	Photosomes	Membranous organelles	Histology, fluorescence and bioluminescence correlation[3]
Arthropoda, Insecta			
Photuris sp.	Photocyte vesicles	Membranous organelles	Histology, fluorescence and bioluminescence correlation[4,5]
Mollusca, Cephalopoda			
Watasenia scintillans Berry, 1911	Rod-like crystals	Cytoplasmic crystals	Microsources isolation, electron microscopy[6]
Echinodermata			
Amphipholis squamata Delle Chiaje, 1828	Cytoplasmic vesicles	Membranous organelles	Ultrastructural changes during luminous event[7]
Chordata, Osteichthyes			
Porichthys notatus Girard, 1854	Photocyte vesicles	Membranous organelles	Histology, fluorescence and bioluminescence correlation in larval stage[8] Ultrastructural changes during luminous event[9]
Chordata, Chondrichthyes			
Etmopterus spinax Linnaeus, 1758	Glowons	Cytoplasmic granular structures	Histology, fluorescence and bioluminescence correlation[10,11]

[1] DeSa et al. (1963);
[2] Anderson and Cormier (1973);
[3] Bassot and Bilbaut (1977);
[4] Hanson et al. (1969);
[5] Smalley et al. (1980);
[6] Hamanaka et al. (2011);
[7] Deheyn et al. (2000); [8] Anctil (1977); [9] Anctil (1979);
[10] Claes and Mallefet (2008);
[11] Renwart et al. (2014)

granular inclusions would therefore be the shark's microsources, as already proposed (Renwart et al. 2014). Given the particular hormone-dependent slow kinetics of shark luminescence, we propose here the term "glowons" for these particles, by analogy with the dinoflagellate's "scintillons", which are among the few other microsources lacking a surrounding membrane (Table 1).

In prolactin-stimulated photocytes, granular inclusions display either a homogeneous sparse distribution (Fig. 3a–c) or, in a few cases (mainly at *PRL max*), a heterogeneous distribution in which they form aggregations (clusters) of variable size (Fig. 3d, e). Since each investigated photocyte presented a unique combination of these two distribution types, we were not able to demonstrate whether these distinct morphologies represented chronological stages of the light-emission process. However, since clustered distributions of granular inclusions are mainly found at *PRL max*, they might represent a key step of the light production mechanism. The involvement of endoplasmic reticulum (ER) in bioluminescent reactions has been proved in several organisms, e.g. the brittle star *A. squamata*, whose ER extends during light emission (Deheyn et al. 2000) and the scale worms (Polynoidae) in which ER forms a complex network building the microsources (the photosomes) and bears the protein of the bioluminescent reaction (Bassot and Nicolas 1987; Wilson and Hastings 1998). The ER observed in some excited photocytes of *E. spinax* might play a role in luminescence metabolism.

In addition to their action inside the granular area, hormones rearrange the pigmentation of the iris-like structure of photophores in order to mechanically control the light reaching outside. Although this capability has already been demonstrated (Claes and Mallefet 2010b), our micrographs allowed showing this process at the cellular level. After stimulation, melanosomes from the iris-like structure retract their cytoplasmic projections from the photophore centre, which allow more light to pass through the lens and to be recorded from the luminometer (note that light is recorded from the whole skin patch—i.e. from numerous photophores—while ultrastructural changes are studied at the photophore level).

In conclusion, this study aimed to improve our understanding of the light-emission process of the deep-sea shark *E. spinax* thanks to a dynamic morphological approach. We highlighted ultrastructural changes in the photocytes and in the pigmented cells of the iris-like structure during hormonally induced light events. In particular, our results support previous hypothesis following which granular inclusions were the microsources of the lanternshark photophores. A new term ("glowon") has been proposed to characterize this novel intracellular membrane-free particle that produces a long-lasting glow under hormonal stimulation. Further research should investigate the chemical nature of *E. spinax*'s luminous system to elucidate its intracellular distribution and dynamics, in relation to glowon morphological changes.

Acknowledgments This work was supported by a grant from the Fonds de la Recherche Scientifique (FRS-FNRS, Belgium) to M.R. and a grant from the Fonds de la Recherche Fondamentale Collective (FRFC—2.4525.12). J.D., P.F., J.M.C. and J.M. are, respectively, Research Fellow, Research Director, Postdoctoral Researcher and Research Associate of the FRS-FNRS. We would like to thank A. Aadnesen, manager of the Espegrend Marine Biological Station (University of Bergen, Norway) where animals were kept, and T. Sorlie for the help during field collections. This paper is a contribution to the Biodiversity Research Center (BDIV) and to the Centre Interuniversitaire de Biologie Marine (CIBIM).

References

Anctil M (1977) Development of bioluminescence and photophores in the midshipman fish, *Porichthys notatus*. J Morphol 151:363–396

Anctil M (1979) Ultrastructural correlates of luminescence in *Porichthys* photophores. I. Effects of spinal cord stimulation and exogenous noradrenaline. Rev Can Biol 38:67–80

Anderson JM, Cormier MJ (1973) Lumisomes, the cellular site of bioluminescence in coelenterates. J Biol Chem 248:2937–2943

Bassot J-M, Bilbaut A (1977) Bioluminescence des élytres d'*Acholoe*. IV. Luminescence et fluorescence des photosomes. Biol Cellulaire 28:163–168

Bassot J-M, Nicolas G (1987) An optional dyadic junctional complex revealed by fast-freeze fixation in the bioluminescent system of the scale worm. J Cell Biol 105:2245–2256

Bernal D, Donley JM, Shadwick RE, Syme DA (2005) Mammal-like muscles power swimming in a cold-water shark. Nature 437:1349–1352

Claes JM, Mallefet J (2008) Early development of bioluminescence suggests camouflage by counter-illumination in the velvet belly lantern shark *Etmopterus spinax* (Squaloidea: Etmopteridae). J Fish Biol 73:1337–1350

Claes JM, Mallefet J (2009a) Bioluminescence of sharks: first synthesis. In: Meyer-Rochow VB (ed) Bioluminescence in focus—a collection of illuminating essays. Research Signpost, Kerala, pp 51–65

Claes JM, Mallefet J (2009b) Hormonal control of luminescence from lantern shark (*Etmopterus spinax*) photophores. J Exp Biol 212:3684–3692

Claes JM, Mallefet J (2010a) Functional physiology of lantern shark (*Etmopterus spinax*) luminescent pattern: differential hormonal regulation of luminous zones. J Exp Biol 213:1852–1858

Claes JM, Mallefet J (2010b) The lantern shark's light switch: turning shallow water crypsis into midwater camouflage. Biol Lett 6:685–687

Claes JM, Aksnes DL, Mallefet J (2010a) Phantom hunter of the fjords: camouflage by counterillumination in a shark (*Etmopterus spinax*). J Exp Mar Biol Ecol 388:28–32

Claes JM, Krönström J, Holmgren S, Mallefet J (2010b) Nitric oxide in the control of luminescence from lantern shark (*Etmopterus spinax*) photophores. J Exp Biol 213:3005–3011

Claes JM, Krönström J, Holmgren S, Mallefet J (2011) GABA inhibition of luminescence from lantern shark (*Etmopterus spinax*) photophores. Comp Biochem Physiol 153C:231–236

Claes JM, Dean MN, Nilsson D-E, Hart NS, Mallefet J (2013) A deepwater fish with 'lightsabers'—dorsal spine-associated luminescence in a counterilluminating lanternshark. Sci Rep 3:1308

Claes JM, Nilsson D-E, Straube N, Collin SP, Mallefet J (2014) Isoluminance counterillumination drove bioluminescent shark radiation. Sci Rep 4:4328

Deheyn D, Mallefet J, Jangoux M (2000) Cytological changes during bioluminescence production in dissociated photocytes from the ophiuroid *Amphipholis squamata* (Echinodermata). Cell Tissue Res 299:115–128

DeSa R, Hastings JW, Vatter AE (1963) "Crystalline" particles: an organized subcellular bioluminescent system. Science 141: 1269–1270

Ebert DA, Fowler SL, Compagno LJ (2013) Sharks of the world: a fully illustrated guide. Wild Nature Press, Plymouth

Hamanaka T, Michinomae M, Seidou M, Miura K, Inoue K, Kito Y (2011) Luciferase activity of the intracellular microcrystal of the firefly squid, *Watasenia scintillans*. FEBS Lett 585:2735–2738

Hanson FE, Miller J, Reynolds GT (1969) Subunit coordination in the firefly light organ. Biol Bull 137:447–464

Renwart M, Delroisse J, Claes JM, Mallefet J (2014) Ultrastructural organization of lantern shark (*Etmopterus spinax* Linnaeus, 1758) photophores. Zoomorphology. doi:10.1007/s00435-014-0230-y

Shimomura O (2006) Bioluminescence: chemical principles and methods. World Scientific, Singapore

Shimomura O, Flood PR (1998) Luciferase of the scyphozoan medusa *Periphylla periphylla*. Biol Bull 194:244–252

Smalley KN, Tarwater DE, Davidson TL (1980) Localization of fluorescent compounds in the firefly light organ. J Histochem Cytochem 28:323–329

Straube N, Iglésias SP, Sellos DY, Kriwet J, Schliewen UK (2010) Molecular phylogeny and node time estimation of bioluminescent Lantern Sharks (Elasmobranchii: Etmopteridae). Mol Phylogenet Evol 56:905–917

Widder EA, Latz MI, Herring PJ, Case JF (1984) Far red bioluminescence from two deep-sea fishes. Science 225:512–514

Wilson T, Hastings JW (1998) Bioluminescence. Annu Rev Cell Dev Biol 14:197–230